Towards Zero-Touch Optical Multiband Networking with the OCATA Optical Time Domain Digital Twin

Prasunika Khare, Sadegh Ghasrizadeh, Mariano Devigili, Marc Ruiz, and Luis Velasco*
Optical Communications Group (GCO), Universitat Politècnica de Catalunya (UPC), Barcelona, Spain;
**e-mail: luis.velasco@upc.edu*

ABSTRACT
Optical in-phase and quadrature (IQ) constellations enclose valuable information regarding the optical elements traversed by the optical signal. Such information can be extracted and exploited by algorithms and models within an optical layer digital twin. In this paper, we focus on their use for accurate quality of transmission (QoT) estimation in multiband optical transmission. Results from simulation show noticeable accuracy.
Keywords: Digital twin; QoT estimation; multiband optical networks

1. INTRODUCTION

Digital twins have been proposed as a key tool for network automation and zero-touch networking (ZTN), as they can provide a holistic representation of the network with high accuracy and, simultaneously, low computational complexity. A digital twin should generate, among others, expected signals and Quality of Transmission (QoT) that can be compared with those obtained from the network. In that way, deviations between the observed and the expectations can be detected and used for, e.g., soft-failure and anomaly detection [1], [2]. Several tools can be used to develop digital twins for optical communications to estimate signal's Linear Interference (LI) noise and Non-Linear Interference (NLI) noise powers and thus, the QoT of optical signals. In parallel, Machine Learning (ML) has shown its potential application for network automation [3]. The low computational requirements of ML models for inference, once trained, make ML very attractive to solve hard computational problems.

In our previous paper in [4], we proposed the OCATA optical time domain digital twin based on Deep Neural Networks (DNN) to model how LI and NLI noise from network components (i.e., reconfigurable optical add/drop multiplexers (ROADMs) and optical links) impact in-phase and quadrature (IQ) optical constellations. Such models can be used for multiple network automation applications, specifically: (a) during *lightpath provisioning*, where pre-forward error correction (pre-FEC) bit error rate (BER) prediction can be used to assess the feasibility of the selected route before establishing the lightpath; and (b) during *lightpath operation* for QoT monitoring and failure management purposes.

The work in [5] showed applications of the OCATA time domain digital twin for QoT and failure management. In this paper, we focus on Multiband optical transmission (MB). MB is considered as the next technological evolution in optical WDM transport capable of dealing with the traffic needs of 5G and beyond networks in a cost-effective manner [6]. MB expands the available capacity of optical fibers by enabling transmission within, e.g., the S band, in addition to the already commercially available C or C+L bands. However, because MB involves a large number of optical signals, the complexity of operating such networks increases. Then, we target at extending OCATA to estimate QoT in MB because of its potential to reduce the complexity of operating multiband optical networks thus, paving the way for ZTN in MB.

2. OCATA OPTICAL TIME DOMAIN DIGITAL TWIN

Fig. 1 represents a lightpath in the optical data plane (a) and its OCATA digital twin (b). We assume that every optical node is controlled by a local agent that configures the underlying optical devices and collates telemetry data from them. On top of the architecture, a software-defined networking (SDN) controller connects to the node agents and to a layer modeling the data plane that includes OCATA components: *i*) a model DB with DNN models for the different network components. Different component models are pre-trained for components with different characteristics, like fiber length and type, and number of spans in the case of optical links. Component models propagate input features after being impacted by the impairments of the specific network component being modeled, and produce output features. Such component models can be concatenated to represent end-to-end lightpaths, so the output features from one component model become the input of the next one. Then, creating a digital twin for a lightpath consists in concatenating models for the specific elements in the route of the lightpath; *ii*) a sandbox domain, that is used to compose the models for the end-to-end lightpaths; and *iii*) a set of algorithms that analyze the features of the signals received and compare to those generated by the models.

As an example, Fig. 1 represents a lightpath in the optical data plane and its OCATA digital twin. To reduce complexity, only the features of a few selected constellation points are propagated. Then, a constellation

The research leading to these results has received funding from the European Community through the MSCA MENTOR (G.A. 956713), the European Union's Horizon Europe research and innovation programme SEASON (G.A. 101096120), the MICINN IBON (PID2020-114135RB-I00) and from the ICREA Institution.

979-8-3503-7732-3/24/$31.00 ©2024 IEEE

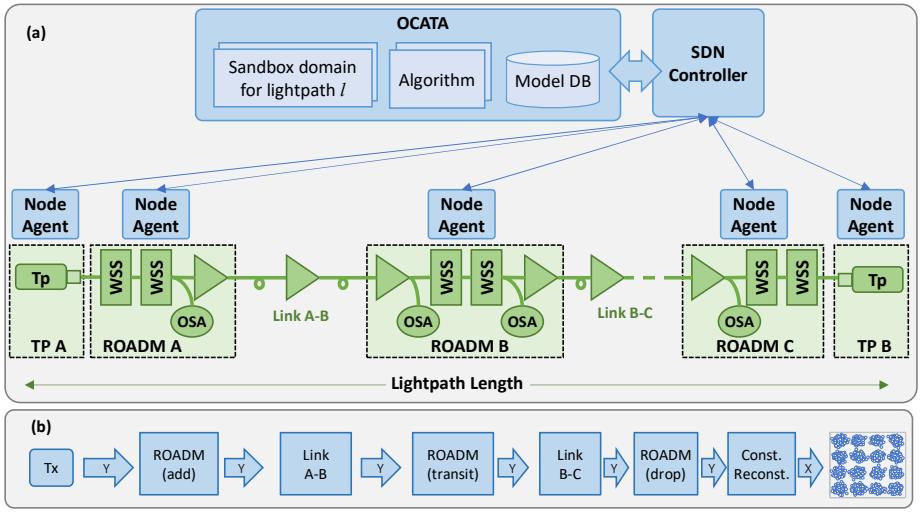

Fig. 1. Architecture and lightpath example (a) and OCATA modeling (b).

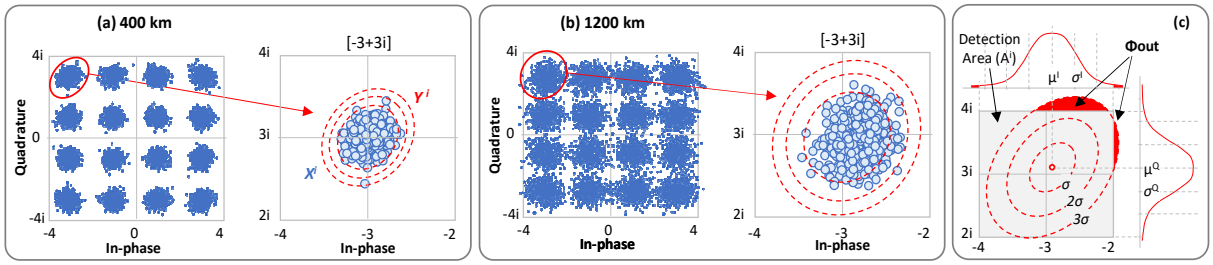

Fig. 2. GMM fitting for feature extraction (FeX) from samples after 400 km (a) and 1200 km (b). Example of *Φout* (c).

reconstruction module generates the features of the non-propagated constellation points based on the received features to complete the IQ optical constellation.

In OCATA, IQ optical constellation samples X are defined by a sequence of symbols $x \in X$, where every symbol belongs to one among m constellation points (CP) in an m-QAM optical signal. Then, samples are summarized as a set of semi-supervised constellation features Y, where vector Y^i defines the features characterizing the CP i. We work under the assumption that dispersion of symbols around constellation point i follow the bi-variate Gaussian distribution characterized by Y^i. Hence, Gaussian Mixture Models (GMM) fitting is used in the feature extraction (FeX) procedure to characterize a given sample X as a set of bivariate Gaussian distributions with one distribution per CP. In consequence, vector $Y^i = [\mu^I, \mu^Q, \sigma^I, \sigma^Q, \sigma^{IQ}]$ includes 5 features representing the I and Q mean position in the constellation (μ) and the I and Q variance and symmetric covariance terms (σ) that the symbols belonging to CP i experience around the mean. For illustrative purposes, Fig. 2a-b reproduce from [5] an example for CP [-3+3i]. The contours represent the different levels of the bi-variate Gaussian distribution that characterize this CP for a given lightpath.

The basic features Y can be extended with additional features. In particular, a new feature denoted Φout^i was defined in [5] that computes the probability that a symbol initially transmitted in constellation point i is detected in the Rx out of the *detection area* of such constellation point, denoted as A^i. For the sake of clarity, Fig. 2c reproduced from [5] an example of Φout^i for CP [-3+3i]. As before, contours are used to represent the different levels of the bi-variate Gaussian distribution characterize this CP, while univariate marginal distributions are provided for both I and Q axes. The area highlighted in red in both bi-variate and marginal distributions represent the region that falls out of A^i, i.e., the square delimited by vertices (-4+4i) and (-2+2i). Hence, Φout^i was formally defined as follows:

$$\Phi out^i = 1 - P\left(x \subset A^i \middle| x \sim N(Y^i)\right) \quad (1)$$

Note that the estimated pre-FEC BER can be computed based on Φout^i for all the CPs, e.g., assuming equal probability of the symbols.

In addition, the function $diff(X_r, X_e)$ was proposed to compare received signals (X_r) and the expected ones (X_e), by computing the Euclidean distance of the difference between the features extracted from X_r and the expected ones (eq. (2)). An application case for is failure detection.

$$diff_Y(X_r, X_e) = \|Y_r - Y_e\|_2 \quad (2)$$

3. QoT ESTIMATION AND FAILURE DETECTION IN MB

One important issue to consider when planning MB is the stimulated Raman scattering (SRS) effect, which increases nonlinearities. In this regard, some authors have already proposed models for taking into account the SRS effect in the calculation of the nonlinear interference [7]. However, tools not only for accurate but also fast QoT estimation of *lightpaths* on MB networks are needed for the MB ZTN. In particular, in this section we study the accuracy of OCATA for fast QoT estimation in MB.

To that end, we used the MATLAB-based simulator of a coherent MB (C+L+S) WDM system developed in [8]. IQ constellations for 16QAM@32GBd signals shaped by a root-raised cosine filter with a 0.06 roll-off-factor were generated. For the C+L+S system, we consider 337 optical channels, with 50 GHz channel spacing for full spectrum usage; ranges of channels for the S, C and L bands are [1-128], [129-215], [216-337].

Pseudorandom binary sequences of length 2^{16} are used as input of every channel. The signal is propagated through 80-km spans of standard single mode fiber, with a launch power of 0 dBm. Gain flattening filters are used at the end of each fiber span to compensate for the power tilt induced by the SRS effect. The attenuation factor, dispersion parameter and nonlinear (gamma) varies with frequency. The SRS Raman factor considered is 0.245. Spans are modeled by solving the nonlinear Schrödinger equation using the Runge-Kutta method (see [8]), whereas ideal inline OAs are modelled as EDFAs and TDFAs. An adaptive step size algorithm is also included to further reduce the computation time required by the Runge-Kutta method. Finally, at the Rx, a Digital Signal Processing (DSP) block performs ideal chromatic dispersion compensation and phase recovery. Table 1 summarizes the configurations used in the MB transmission simulator.

Table 1. Parameters of the MB simulator

	S Band	C Band	L Band
Wavelength range[nm]	1481.7-1530.1	1530.1-1564.8	1564.8-1616.7
Bandwidth [THz]	6.19	4.35	5.76
Num of Channels	128 [1-128]	87 [129-215]	122 [216-337]
Type of Amplifier	TDFA	EDFA	EDFA
Amplifier Noise Figure	5		
Non-Linear coefficient Dispersion, Attenuation	Vary with frequency		
Launch Power	0 dBm		

We used the MB transmission simulator to generate datasets for training, testing, and validating DNN models that propagate input features for different number of spans. Specifically, we focus on channels 1, 194, and 337.

To validate the MB transmission simulator, we compared the results of MB transmission to those obtained with the simulator for the C-band which considers 11 channels only, as the latter was experimentally validated in [9]. To that end, the pre-FEC BER of the signals is calculated after each span; results for BER as a function of the distance and as a function of the channel are presented in Fig. 3. Fig. 3a shows the BER for a reference channel in the C band and Fig. 3b for three channels (1, 194, and 337) in the C+L+S bands. We observe that distances in the order of 480 km (6 spans) result in a pre-FEC BER exceeding a threshold of 10-2 in the case of MB transmission, while in the case of the C-band the pre-FEC BER is below the threshold even after 13 spans (1,040 km).

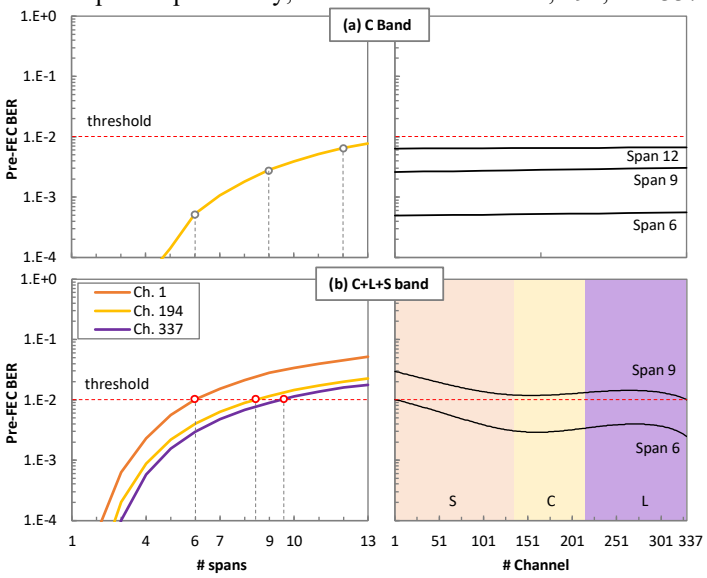

Fig. 3. BER vs distance and vs wavelength for C (a) and C+L+S (b) bands

In addition, we notice different performance for the different bands, being the S band the one that is more affected by the physical layer impairments and supports shortest distances.

Let us now see the effects on the resulting IQ optical constellations of the channels. In particular, we analyze IQ constellations after three spans and compare the results from the simulator and from our modeling approach presented previously. Fig. 4a presents the obtained bivariate Gaussian distributions of IQ constellation of the selected channels and Fig. 4b zooms in two CPs, one interior and the other exterior. Contours correspond to levels 0.1 and 0.01 of the variance of the respective Gaussian distributions. Strong similarities between both distributions are evident, which validates the proposed modelling approach. It is interesting to observe the changes of the constellations for the different channels, which is more noticeable in the external CPs. In particular, we observe a higher impact of nonlinear fiber propagation for the channel in the S band than for the ones in the C and L bands. Specifically, we observe that in the case of CP [-3+3i] for channel 1, part of the contours exceeds the detection area for that CP, which is a clear indication of high pre-FEC BER. A similar behavior, although with much smaller

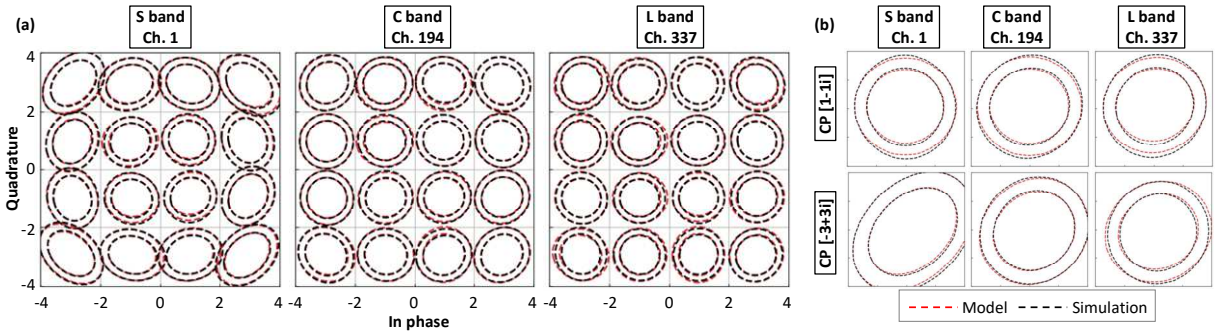

Fig. 4. Comparison for the selected channels in S, C and L bands from the simulator vs DNN models: (a) IQ constellations and (b) detail of two CPs.

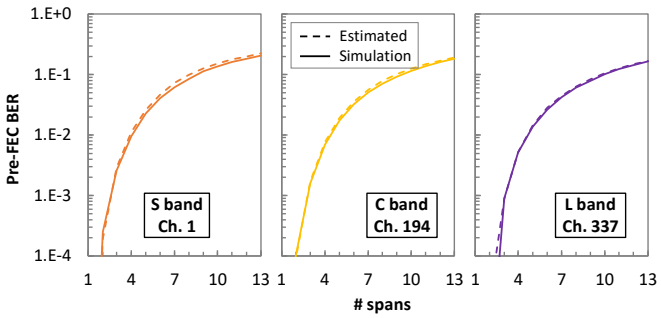

Fig. 5. Pre-FEC BER estimated vs MB simulator.

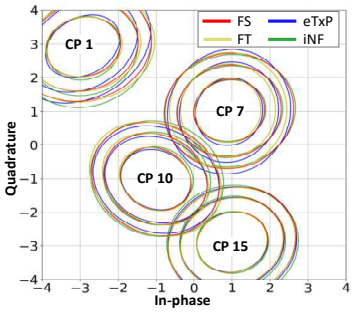

Fig. 6. CPs of signals affected by failures

magnitude since all contours are still inside the detection area is observed for channel 194, which indicates lower pre-FEC BER.

We now focus on estimating the pre-FEC BER of the signals based on the probability Φ^{i}_{out} on MB transmission. Fig. 5 compares the estimated pre-FEC BER with the value from the MB simulator. The accuracy of the estimation is clear for three selected channels and all the considered number of spans, which validates OCATA for MB transmission.

Finally, let us consider signals that are affected by failures. Several possible soft-failure affecting a lightpath are considered: (a) transmitter, e.g., an extra gain in its booster amplifier leading to an extra transmission power (eTxP); (b) increased noise figure on an EDFA (iNF); and (c) a failure in an optical filter that produces filter tightening (FT) or filter shift (FS) on the optical signal. Although some of the failures can be detected and identified by analyzing the optical spectrum of the signal only (see [1], [2]), here we target at showing the effects of those failures in the time domain, which might enhance such detection by frequency domain analysis. Fig. 6 shows the impact of the different failures at their higher magnitude on the bivariate distributions of the selected CPs (σ, 2σ, and 3σ levels are represented). We observe that the impact of the soft-failures on the distributions is small and we cannot observe changes that allow to clearly distinguish one failure type from the others. However, a more in-depth analysis can reveal some useful patterns for failure classification.

4. CONCLUSIONS

Models for MB transmission have been proposed to extend the OCATA digital twin. Deep Neural Networks models propagate features related to IQ constellations. Specifically, features from 3 channels, for C, L, and S bands are selected. Results show remarkable accuracy of the pre-FEC BER computed from the reconstructed IQ optical constellations, which has a wide number of applications for network operation. Finally, the impact of different failures on IQ constellations is presented to show that the optical time domain can be used for failure management purposes.

REFERENCES

[1] B. Shariati *et al*., "Learning from the Optical Spectrum: Failure Detection and Identification [Invited]," JLT, 2019.
[2] A. P. Vela *et al*., "Soft Failure Localization during Commissioning Testing and Lightpath Operation [Invited]," JOCN, 2018.
[3] D. Rafique, L. Velasco, "Machine Learning for Optical Network Automation: Overview, Architecture and Applications," JOCN, 2018.
[4] D. Sequeira *et al*., "OCATA: a deep-learning-based digital twin for the optical time domain," JOCN, 2023.
[5] M. Devigili *et al*., "Applications of the OCATA Time Domain Digital Twin: from QoT Estimation to Failure Management," JOCN, 2024.
[6] L. Velasco *et al*., "Introduction to the JOCN Special Issue on Advances in Multi-Band Optical Networks," JOCN 2023.
[7] A. Souza *et al*., "Comparison of fast quality of transmission estimation methods for C+L+S optical systems," JOCN 2023.
[8] P. Khare *et al*., "SSMS: A Split Step MultiBand Simulation Software," ICTON, 2023.
[9] M. Devigili *et al*., "Experimental Validation of Deep Learning-based Models for Optical Time Domain Analysis," CLEO, 2023.